193-nm Immersion Photomask Image Placement in Exposure Tools

Eric Cotte*[a], Benjamin Alles[b], Timo Wandel[a], Gunter Antesberger[a], Silvio Teuber[a],
Manuel Vorwerk[c], Andreas Frangen[c], and Frank Katzwinkel[c]
[a] Advanced Mask Technology Center (AMTC), Rähnitzer Allee 9, 01109 Dresden (Germany)
[b] TU München, Boltzmannstr. 3, 85747 Garching (Germany)
[c] Infineon Technologies AG, Königsbrückerstr. 180, 01099 Dresden (Germany)

ABSTRACT

In case drastic changes need to be made to tool configurations or blank specifications, it is important to know as early as possible under which conditions the tight image placement requirements of future lithography nodes can be achieved. Modeling, such as finite element simulations, can help predict the magnitude of structural and thermal effects before actual manufacturing issues occur, and basic experiments using current tools can readily be conducted to verify the predicted results or perform feasibility tests for future nodes. Using numerical simulations, experimental mask registration, and printing data, the effects on image placement of stressed layer patterning, blank dimensional and material tolerances, as well as charging during e-beam writing were investigated for current mask blank specifications. This provides an understanding of the areas that require more work for image placement error budgets to be met and to insure the viability of optical lithography for future nodes.

Keywords: optical mask, registration, charging, mask chucking, overlay, wafer exposure.

1. INTRODUCTION

For the successful extension of 193-nm immersion lithography down to and below the 45-nm node, mask image placement and wafer overlay errors are a concern.[1] Currently, overlay at the wafer level is specified to be no larger than 19% of the mask half-pitch. From this overlay error budget, roughly 30% is allocated to mask placement errors. The maximum image placement at the mask level allowed is half the maximum overlay. As linear parts of the placement errors are correctible in exposure tools, mask image placement is specified after multi-point alignment and removal of isotropic magnification. Thus, the maximum allowable wafer overlay error at the 45-nm node is 8.0 nm, and the maximum permitted mask image placement error is 4.8 nm.

Year of Production	*2005*	*2006*	*2007*	*2008*	*2009*	*2010*	*2011*	*2012*	*2013*
DRAM ½ Pitch (nm) (contacted)	*80*	*70*	*65*	*57*	*50*	*45*	*40*	*36*	*32*
Overlay (3 sigma) (nm)	*15*	*13*	*11*	*10*	*9*	*8*	*7*	*6*	*6*
Mask magnification	**4**	**4**	**4**	**4**	**4**	**4**	**4**	**4**	**4**
Image placement (nm, multi-point)	**9**	**8**	**7**	**6.1**	**5.4**	**4.8**	**4.3**	**3.8**	**3.4**

Fig. 1. Excerpt of 2005 ITRS document, focusing on image placement issues.[1]

Some well-known sources of pattern distortions are the mask writer stage and beam positioning error, structuring of stressed layers, and mask heating during writing as well as under 193-nm light exposure. This paper focuses on additional causes of mask distortions, namely blank charging during electron-beam writing, as well as tolerances in substrate dimensions and material properties, which influence the structural response of masks under gravity in various tools. Additionally, the sources of overlay errors due to masks and tools in wafer fabs are mentioned.

*email: Eric.Cotte@amtc-dresden.com

The outline of this paper is as follow: sources of image placement error are presented, starting with well-known or oft-published effects, then effects that are not so well-known or underestimated according to the authors of this paper, and effects occurring during mask usage in the wafer fab. Finally, each effect will be classified as noise or systematic, and according to whether solutions are already known for its reduction or correction, thus pointing to the main issues demanding research and development work for future nodes.

2. WELL-KNOWN EFFECTS

2.1 Writer positioning error

An obvious source of registration error is the mask writer stage and beam positioning error. This error can be monitored and represents the pattern generator's best registration capability. Tuning a mask writer consists not only in minimizing this positioning error, also referred to as footprint, but also in making sure this footprint is not systematic. To test this, dedicated testmasks can be written and their registration can be analyzed to determine if this placement error is systematic or merely noise. In particular, the distribution of the displacements can be compared to a Gaussian distribution, characteristic of noise, or a statistical evaluation can be used, such as a QQ plot representation. As an example, Fig. 2 (a) illustrates the distribution of x-displacements obtained with a particular mask writer, called generation I in this paper, on which a Gaussian curve is superimposed. In this example, the writer used was a 50kV electron-beam system, and the distribution is Gaussian, implying that the tool footprint has no systematic part. The standard deviation of the distribution is representative of the tool's placement capability. This e-beam writer can be compared to tools of later generations, as depicted in Figs. 2 (b) and (c). Improvements in image placement are visible via the reduction of standard deviation, while the stage positioning error remains non-systematic.

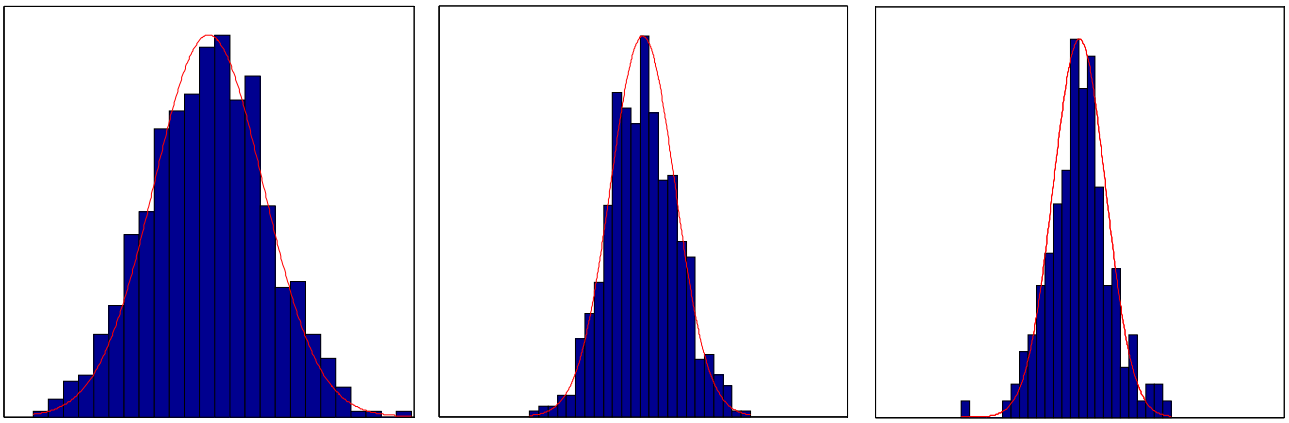

Fig. 2. Histogram of writer placement errors in X, for an e-beam of generation (a) I, (b) II, and (c) III. All scales identical.

As already mentioned, a QQ plot is another way of testing if the distribution of the writer stage placement is Gaussian, and Fig. 3 (a) is a QQ plot of the x-displacements. For this example, a well-tuned e-beam of generation I was used and the straight line obtained is characteristic of a Gaussian distribution. As a comparison, the histogram of the distribution of the placement for a poorly-tuned tool can be shown in Fig. 3 (c), and the corresponding QQ plot in Fig. 3 (b). Both figures show that the stage placement error was not Gaussian-distributed in this case.

It must be noted that the histograms and QQ plots are not only representative of pattern generator placement distributions, but also of the registration measurement capability, i.e., the distribution of the measurement errors, which will be addressed in a later section. Another detail of note is that the generation III e-beam writer hasn't been in use as long as the other writers, which explains why it does not yet bring as great an improvement as the previous tool did.

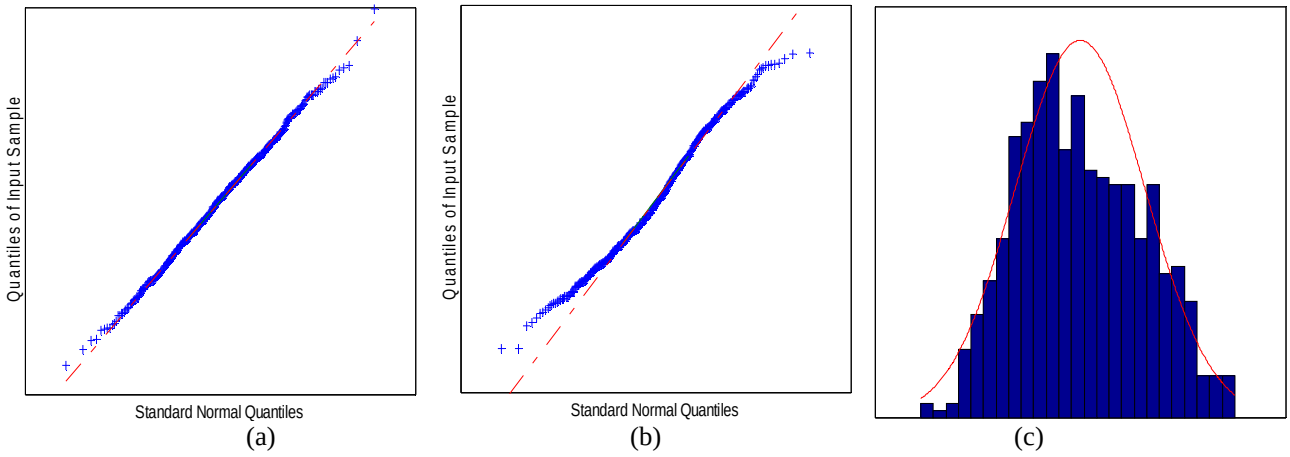

Fig. 3. QQ plot for placement errors in X for (a) a well-tuned e-beam writer of generation I and (b) a poorly-tuned e-beam writer of generation II, as well as (c) a histogram of placement errors in X for a poorly-tuned e-beam writer of generation II.

2.2 Absorber etching

Another well-known source of image placement error is the selective etching of stressed layers, sometimes referred to as pattern transfer from the resist to the absorber. This effect is easily evidenced by measuring registration first on the resist and later on the absorber: the overlay of these two measurements is the contribution to mask distortions of absorber etching. A simple analytical formula can be used to link the out-of-plane displacements of a mask due to the uniform etching of a layer: Stoney's equation.[2] On the other hand, the calculation of a mask's in-plane displacements due to the local etching of a layer requires the use of finite element modeling.

Multiple articles have been written on the subject of pattern transfer for optical masks, illustrating the order of magnitude of this effect depending on the mask stack (absorber thickness and stress) and mask design.[3,4] In particular, mask patterning distortions were shown to vary linearly with layer stress. Additionally, numerical simulations were performed for EUV masks, due to their even more stringent image placement requirements.[5,6] Such models were put in use for the correction of simple patterning effects, for designs consisting of etching away absorber in a large square or rectangular region.[7] Finally, models linking layer stress values and image placement magnitudes were experimentally verified, and some absorber layers were characterized.[8]

Examples are shown here to illustrate this effect and the fact that it can be modeled, as well as its dependence on mask design and materials properties (layer stress). Figure 4 (a) is a plot of the experimentally-obtained mask distortions due to the etching of a MoSi absorber in two opposite quadrants (top-left and bottom-right). The inwards-directed distortions are characteristic of the etching of a compressive layer such as MoSi. Figure 4 (b) is a plot of the numerically-calculated mask distortions for the etching of the same design, showing good qualitative agreement with the experimental results (the overlay of these two results is within the accuracy of the registration measurement tool). From the comparison of results of such experiments and models, stress values can be extracted for various layers, which can then be used to predict distortions due to the patterning of other designs.

Similarly, Figs. 5 (a) and (b) illustrate the distortions due to the patterning of a large L-shaped structure on a Cr layer, without any correction and with scale and orthogonality correction applied, respectively. The edges of the L structure are marked on the plot in Fig. 5 (b). The results in Figs. 4 and 5 show that stress effects are material- as well as layout-dependent, systematic, and that they can be modeled via finite elements, which could allow to pre-correct for them during mask writing. In addition, new absorber materials with lower stress could be introduced, which would help reduce etching-induced distortions or might render them negligible.[9] Naturally, the introduction of new materials is done cautiously, as it influences other parameters in the mask-making process.

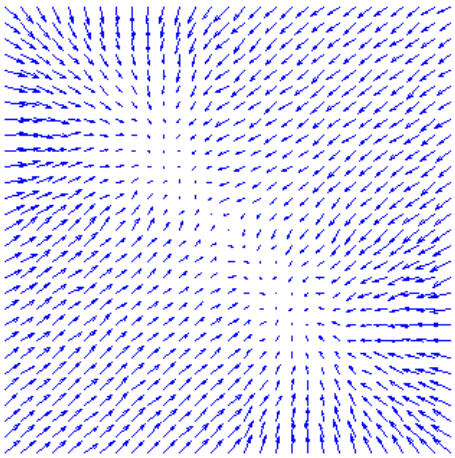

Data Analysis

[nm]	x	y			
Mean	0.00	-0.00	Min	-12.29	-10.08
3 Sigma	18.84	15.13	Max	13.21	10.16

(a)

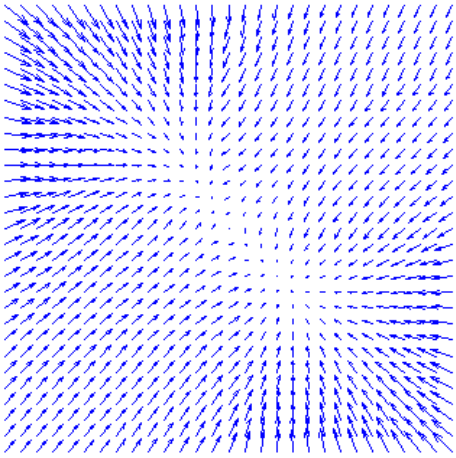

Data Analysis

[nm]	x	y			
Mean	1.25	-0.00	Min	-12.60	-13.10
3 Sigma	18.09	18.32	Max	15.11	12.81

(b)

Fig. 4. Mask distortions obtained (a) experimentally and (b) numerically due to the local etching of a MoSi layer in its upper-left and lower-right quadrants. No correction applied besides multipoint alignment.

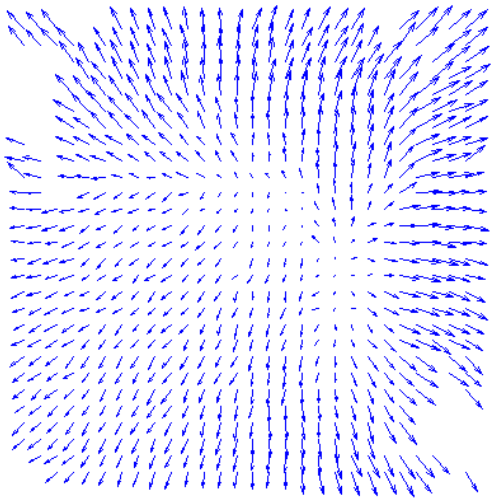

Data Analysis

[nm]	x	y			
Mean	-0.00	-0.00	Min	-10.48	-13.14
3 Sigma	18.06	21.68	Max	14.18	15.55

(a)

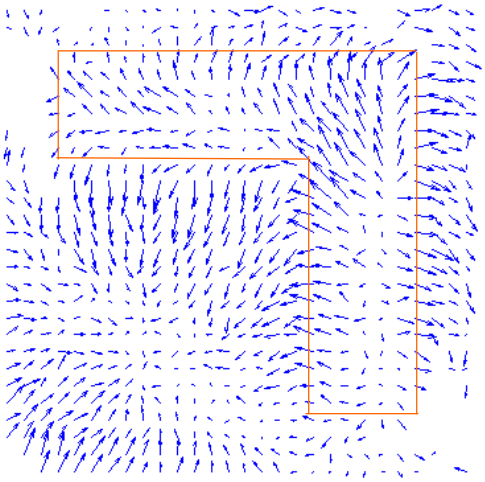

Data Analysis

[nm]	x	y			
Mean	-0.00	-0.00	Min	-6.51	-7.49
3 Sigma	7.21	7.67	Max	6.32	7.34

(b)

Fig. 5. Experimentally obtained mask distortions due to the etching of a L-shaped pattern in a Cr layer, (a) before and (b) after scale and orthogonality corrections.

2.3 Mask writer heating

Optical mask heating under pattern generator exposure was first studied numerically, experimentally, and analytically with the focus on resist heating, to investigate chemical changes in the resist, such as its development rate and impact on critical dimensions.[10-12] Eventually, the studies of heating were extended to its effect on the substrate, in particular the displacements caused by the thermal loads.[13] It was numerically calculated that substrates could heat up by a few degrees at most (in comparison to resists that can heat up to hundreds of degrees), resulting in tens of nanometers of placement error, which was later confirmed via independent finite element simulations.[14] Different parameters and writing styles were then investigated, such as the influence of multipass writing, and a 4-pass writing sequence was calculated to induce a 0.4 K temperature rise and 6.2 nm maximum distortions.[15] Up to this point, no magnification correction was applied to the reported distortions. In a later study, single-pass writing was reported to lead to heating by 1.0 K, resulting in 10.0 nm distortions before the application of corrections, and 4.0 nm after magnification correction.[4] However, multi-point alignment was not applied to the results, which could have greatly reduced the distortions. In addition, a higher dose was used in the models than the ones employed with current resists (5 to 7 times higher than current doses) and the writer simulated had a different acceleration voltage, which can lead to believe that the distortions reported were over-estimated. Thus, it is believed that the use of low doses, multipass writing, and the proper alignment and magnification corrections render this effect negligible.

2.4 Measurement accuracy

Another item to take into account in placement error budgets is the accuracy of the tool used for the measurement of mask registration.[16] Three main parameters describe a placement measurement tool's capabilities: short-term repeatability, long-term repeatability, and nominal accuracy. Short-term repeatability of the metrology system is influenced by temperature variations, acoustic vibrations, air turbulence, and pressure variations. Long-term repeatability represents a drift from footprint in time and is influenced by the precision of the mask loading on its 3-point holder. If all metrology tools (within a mask house and in different mask houses) were calibrated via a standard reference, monitoring long-term repeatability would be enough to ensure that the measurement error is acceptable. However, as this is not the case, another parameter must be checked: nominal accuracy, which is a measure of differences in X and Y scales as well as orthogonality of the coordinate system and higher order distortions.

With tightening registration specifications, come tougher requirements on tool accuracy and the need for newer tools. For example, Leica introduced its LMS IPRO 3 in the Summer of 2005, featuring improved temperature control, for both temperature stability and homogeneity, as well as other hardware and software improvements.[17] An overview of the targeted capabilities of this new tool, and a comparison to its predecessor, is given in Table 1.

Table 1. Leica LMS IPRO 2 and 3 registration measurement tool specifications. [17]

	Performance IPRO 2	Target for IPRO 3
Short-term repeatability	2.0 nm	1.3 nm
Long-term repeatability	3.0 nm	2.2 nm
Nominal accuracy	4.0 nm	2.7 nm

A detail to be noted is that these tools measure registration while holding the mask horizontal via a 3-point mount. Therefore, part of the distortions measured are due to gravity acting on the mask. Since these mask sagging distortions are systematic and can easily be modeled, they can be numerically corrected for in order to report the registration of an unconstrained mask. To test the validity of this compensation algorithm, an experiment was run: a mask was measured with and without applying this compensation. The overlay of these results thus represents the effect of gravity, as removed by the algorithm, and is shown in Fig. 6 (a). As a comparison, Fig. 6 (b) is the result of a finite element calculation performed in-house, which is in good agreement with the experimental values (well within the reported tool short-term repeatability). However, given the tightened registration specifications of future lithography nodes, any numerical error in the application of these compensations could be detrimental, as discussed in the next section, focusing on lesser known effects.

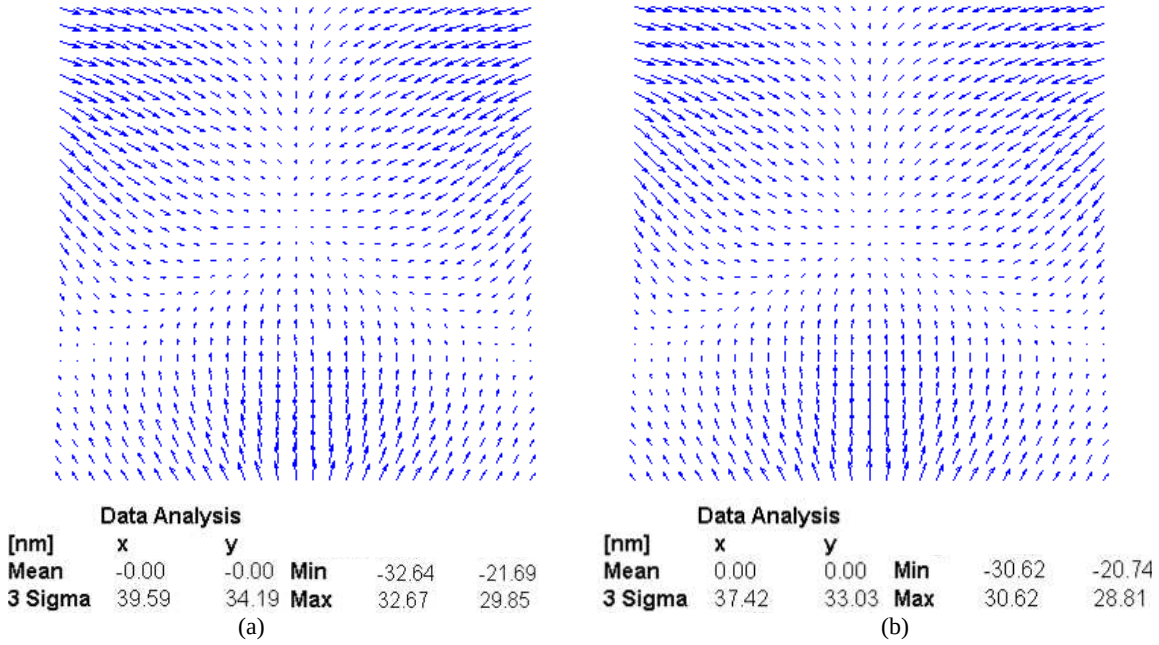

Fig. 6. Registration compensation of gravity effect (a) measured experimentally and (b) computed numerically. No corrections applied besides multipoint alignment.

3. NOT SO WELL-KNOWN EFFECTS

3.1 Influence of substrate properties

The thickness of optical masks is specified by SEMI standards, and a variation of ± 0.1 mm is currently allowed.[18] Such variations influence the mask's behavior under gravity, for example in a 3-point mount, i.e., the amount by which it sags as well as the corresponding in-plane distortions. It was calculated that a ± 0.1 mm thickness variation would induce a ± 0.6 nm variation in the registration, which will not be a trivial amount for future nodes.[1] Therefore, thickness variations from blank to blank and blank thickness non-uniformities might have to be specified more tightly, or measured so that numerical compensations of mask sagging effects can be appropriately adjusted.
Additionally, the elastic modulus of substrates has an influence similar to that of their thickness, and a variation of elastic modulus by ± 1.2 GPa has been calculated to induce a variation in mask registration of ± 0.6 nm. Unlike substrate thickness, elastic modulus values are currently not specified. Therefore, efforts might need to be put into monitoring and eventually specifying blank material properties, as is done for blank dimensions.

3.2 E-beam writer charging effects

Each shot of an e-beam writer induces charging inside the blank. Such charges deflect the next shots of electron beams, which results in misplacement. This interaction between reticle and e-beam is well-known, but its magnitude might be underestimated. Furthermore, no rigorous model for it is currently available beyond the simplified one proposed by Cummings et al.[19] Some work has been put into investigating the effect of charging on critical dimensions, leading to proximity correction models, but does not overlap with registration issues.[20] Placement errors due to low-energy electron beams have been studied, but the effects are much larger for these tools (up to hundreds of nanometers when writing on Quartz substrates), due to the lower speed of the electrons at low voltage.[21] Some experiments have been performed with high-voltage e-beams and have evidenced the beam deflection induced by charges in optical masks.[19, 22]
A simple experiment was run in-house to verify and attempt to characterize such effects: a reference grid of crosses was

first patterned, followed by the design shown in Fig. 7 (a), which was exposed with an e-beam writer along with a second set of registration crosses. The overlay of registration data from these two sets of placement marks, shown in Fig. 7 (b) after application of standard corrections, is thus representative of charging effects due to the large L-shaped region. It must of course be noted that this overlay also contains errors due to the stage positioning error as well as the measurement accuracy, both of which are randomly-distributed for well-tuned tools. Therefore, the systematic effects seen can be attributed to charging only, unless studies of e-beam heating have grossly under-estimated thermal effects. A comparison with the results in Fig. 5 (b), which represent stress effects induced by the same layout, shows that charging effects can be as large, or even larger, than stress effects. This experiment was conducted with single-pass writing, which is not a standard practice anymore and tends to increase charging and heating effects, but their magnitude makes it clear that they need to be understood, and possibly modeled and corrected for. To check models advanced in previous articles and try to understand this effect, distortions were also monitored in the denser array of crosses marked in Fig. 7 (a), and the results are shown in Fig. 8 without correction.

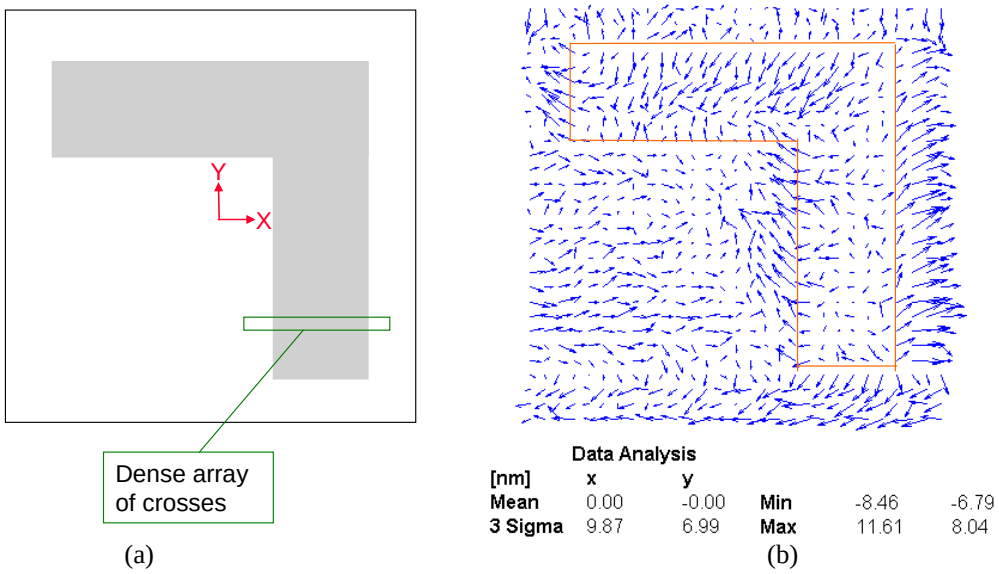

Fig. 7. (a) L-shaped pattern and (b) corresponding charging-induced distortions after scale and orthogonality correction.

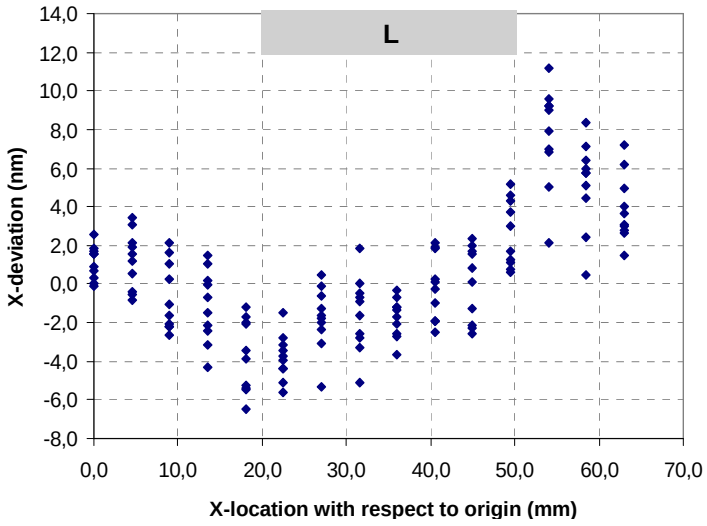

Fig. 8. Plot of the charging-induced x-distortions along the x-axis, uncorrected, in the dense array of crosses shown in Fig. 7 (a).

.
Like Fig. 7 (b), this plot of the x-distortions illustrates the deflection of electrons by charges trapped inside the substrate. More work is required to come up with a model and verify it. Analogous to stress effects, there are also possibilities to reduce or eliminate this effect via the use of specific materials. Charge-dissipating layers have been shown to reduce placement errors by preventing charging and the corresponding deflections.[22, 23] As with new absorbers, the same caution surrounds the introduction of new materials and new chemistries

4. WAFER FAB EFFECTS

4.1 Scanner heating

Masks can heat up during exposure at 193-nm wavelength, leading to temporary distortions that contribute to the overlay errors. As for mask writing in an e-beam, finite element studies have been conducted to characterize this heating effect. For 193-nm exposure with a 100 mW/cm^2 input power, Abdo et al. predicted a maximum temperature rise of 1.2 K and corresponding maximum distortions of 29 nm at the mask level, at steady state and before the application of magnification correction.[24] The distortions at steady state can be used to calculate a worst case of overlay between a layer written as the exposure tool was just warming up and a layer written after steady state was reached.

In one of the most recent studies, a maximum temperature rise of 1.0 K to 1.2 K, depending on the resist sensitivity and scanning speed, was calculated for an input power on the reticle of 100 mW/cm^2. These temperature changes corresponded to maximum distortions of 20 nm to 30 nm before the application of magnification corrections.[25] The distortions after corrections were 12 nm to 16 nm for isotropic magnification corrections and 4 nm to 5 nm for orthotropic corrections. It must be noted that in both of these papers the structural boundary conditions were as follows: full chucking, i.e. no displacements allowed, in the x, y, and z directions on both sides of the mask.

In the most recent study, other boundary conditions were used, and various designs, with different Cr coverages, were considered. Maximum temperature rises from 0.5 K to 1.1 K were calculated, depending on layout, resulting in 26 nm to 60 nm maximum distortions.[26] No magnification corrections were applied, and no overlay between two masks was calculated, which could be worth investigating. Also to consider are the boundary conditions employed in the models, as they influence the results. Finally, an experimental verification by wafer fabs and tool vendors is advisable.

4.2 Scanner clamping effects

In an experiment, a mask was exposed with a recent lithography tool. Distortions are shown in Fig. 9, at the mask-level. In this case, no large lens signature was observed, and a good correlation (at least qualitative) can be seen between mask and wafer data. However, the overlay of mask and wafer distortions shows that there are large exposure tool contributions to image placement errors in some regions.

Such exposure tool contributions could possibly be attributed to mask non-flatness if they turn out to be non-repeatable. Indeed, masks are held more rigidly in exposure tools than in e-beam writers and registration tools, and their non-flatness in areas that contact with the chucking system could lead to in-plane distortions. This still needs to be tested, and there is no concrete proof of a mask flatness influence on wafer overlay so far.

More studies are needed to fully understand the effect of mask distortions during their usage.

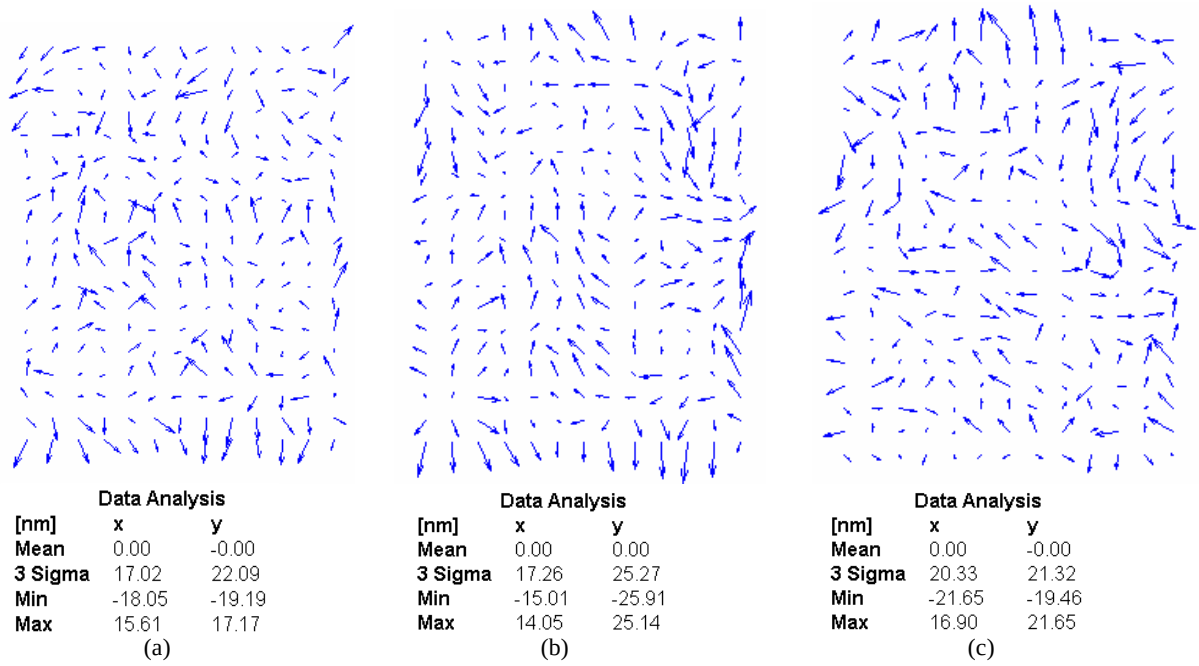

Fig. 9. (a) Mask registration, (b) wafer registration, and (c) overlay of the two at mask level, for a recent exposure tool.

5. SUMMARY AND CONCLUSIONS

A combination of experiments and modeling as well as published results was used to characterize the various effects that come into play in optical mask image placement error budgets. Writer positioning errors are non-systematic for well-tuned tools and reduced with each generation of pattern generator. Absorber etching distortions are systematic, and can be corrected for or reduced with the introduction of new materials. Mask heating during e-beam writing could be negligible due to the use of sensitive resists and multipass writing. Measurement accuracy is non-systematic and improves with newer metrology tools, but monitoring of blank thickness and elastic modulus, as well as appropriate corrections, might be needed in the future. Charging effects can be as large as stress-induced distortions during etching but are not currently understood well enough to be modeled and corrected for. in the near future it might become the main source for registration. More work is required, if the use of charge-dissipating layers proves insufficient or impossible. Finally, mask distortions during their usage should not be underestimated, and more studies are needed to improve layer-to-layer overlay.

ACKNOWLEDGMENTS

AMTC is a joint venture of Infineon, AMD and Toppan Photomasks and gratefully acknowledges the financial support of the German Federal Ministry of Education and Research (BMBF) under contract No. 01M3154A (“Abbildungsmethodiken für nanoelektrische Bauelemente”).

REFERENCES

1. International Technology Roadmap for Semiconductors, 2005 edition, http://public.itrs.net
2. G. Stoney, Proceedings of the Royal Society of London, A82, pp. 172-177, 1909.
3. A. Mikkelson, R. Engelstad, and E. Lovell, "Pattern transfer distortions in optical photomasks," Microelectronic Engineering, Vol. 58-59, pp. 489-495, 2000.
4. A. Mikkelson, A. Abdo, E. Cotte, J. Sohn, R. Engelstad, and E. Lovell, "Mask-related distortions of modified fused silica reticles for 157-nm lithography," SPIE Vol. 4562, pp. 914-925, 2001.
5. A. Mikkelson, R. Engelstad, and E. Lovell, "Determination of image placement accuracy due to EUV mask fabrication procedures," Microelectronic Engineering, Vol. 61-62, pp. 251-255, 2001.
6. E. Cotte, U. Dersch, C. Holfeld, U. Mickan, H. Seitz, T. Leutbecher, and G. Hess, "EUV mask image placement management in writing, registration, and exposure tools," SPIE Vol. 5853, pp. 336-344, 2005.
7. A. Wei, G. Hughes, A. Chalekian, L. Mackey, A. Mikkelson, and R. Engelstad, "Strategies for predictive control of chrome stress-induced registration errors," SPIE Vol. 5040, pp. 182-192, 2003.
8. J. Butschke, U. Buttgereit, E. Cotte, G. Hess, M. Irmscher, and H. Seitz, "Determination of mask layer stress by placement metrology," SPIE Vol. 5992, pp. 1127-1138, 2005.
9. M. Hashimoto, T. Yamada, M. Sakamoto, M. Hara, Y. Ohkubo, and M. Ushida, "Development of new chrome blanks for 65-nm node and beyond," SPIE Vol. 5567, pp. 974-982.
10. N. Eib and R. Kvitek, "Thermal distribution and the effect on resist sensitivity in electron-beam direct write," Journal of Vacuum Science and Technology B, Vol. 7, No. 6, pp. 1502-1506, 1989.
11. E. Kratschmer and T. Groves, "Resist heating effects in 25 and 50 kV e-beam lithography on glass masks," Journal of Vacuum Science and Technology B, Vol. 8, No. 6, pp. 1898-1902, 1990.
12. E. van der Drift, A. Enters, and S. Radelaar, "Thermal effects in high voltage e-beam lithography," Journal of Vacuum Science and Technology B, Vol. 9, No. 6, pp. 3470-3474, 1991.
13. A. Moel and Y. Gomei, "Analysis of mask distortion induced by heating during e-beam writing," SPIE Vol. 2254, pp. 199-205, 1994.
14. B. Shamoun, W. Trybula, R. Engelstad, and E. Lovell, "Effects of material properties on patterning distortions of optical reticles," SPIE Vol. 3546, pp. 214-220, 1998.
15. B. Shamoun, R. Engelstad, and D. Trost, "Assessment of thermal loading-induced distortions in optical photomasks due to E-beam multipass patterning," Journal of Vacuum Science and Technology B, Vol. 16, No. 6, pp. 3558-3562, 1998.
16. M. Chandramouli and Y. Korobko, "Calibration of the registration metrology systems," SPIE Vol. 5567, pp. 1056-1066, 2004.
17. J. Bender, M. Ferber, M., K.-D. Roeth, G. Schlueter, W. Steinberg, G. Scheuring, and F. Hillman, "Actual measurement data obtained on new 65nm generation mask metrology tool set," Proceedings of 21st European Mask and Lithography Conference, pp. 121-124, 2005.
18. SEMI P1-1101 Specification for hard surface photomask substrates.
19. K. Cummings and M. Kiersh, "Charging effects from electron beam lithography," Journal of Vacuum Science and Technology B, Vol. 7, No. 6, pp. 1536-1539, 1989.
20. K. Shirabe, E. Hoshino, and K. Watanabe, "Application of charging dispersing layer to reticle fabrication," SPIE Vol. 3096, pp. 37-41, 1997.
21. K. Satyalakshmi, A. Olkhovets, M. Metzler, C. Harnett, D. Tanenbaum, and H. Craighead, "Charge-induced pattern distortion in low energy electron beam lithography," Journal of Vacuum Science and Technology B, Vol. 18, No. 6, pp. 3122-3125, 2000.
22. J. Hirumi, T. Hayasimoto, and T. Kawabata, "Deflection error due to charge-up effect of reticle substrate," SPIE Vol. 3412, pp. 307-318, 1998.
23. C. Koepernik, J. Butschke, D. Beyer, M. Irmscher, B. Leibold, E. Rausa, R. Plontke, J. Plumhoff, and P. Voehringer, "Alternating aperture phase shift mask process using E-beam lithography for the second level," Photomask Japan, SPIE Vol. 5446, pp. 183-192, 2004.
24. A. Abdo, R. Engelstad, W. Beckman, J. Mitchell, and E. Lovell, "Predicting thermomechanical distortions of optical reticles for 157nm technology," SPIE Vol. 4186, pp. 724-732, 2001.
25. A. Abdo, L. Capodieci, I. Lalovic, and R. Engelstad, "Effect of chrome pattern characteristics on image placement due to the thermomechanical distortions of optical reticles during exposure," Journal of Vacuum Science and Technology B, Vol. 21 No. 6, pp. 3052-3056, 2003.
26. Q. Zhang, K. Poolla, and C. Spanos, "Modeling of mask thermal distortion and its dependency on pattern density," SPIE Vol. 5853 pp. 234-242, 2005.